Electronic structure of Au-induced surface phases on Si(110): LEED and angle-resolved photoemission measurements

Se Hun Kang, Keun Su Kim, and Han Woong Yeom*
Institute of Physics and Applied Physics and Center for Atomic Wires and Layers, Yonsei University, Seoul 120-749, South Korea
(Received 27 May 2008; revised manuscript received 16 July 2008; published 19 August 2008)

Au-induced reconstructions of the Si(110) surface have been studied using low-energy electron diffraction and angle-resolved photoemission (ARP). Low-energy electron diffraction reveals three well-ordered phases: 1×2, 2×5, and $(4,0)\times(\bar{1},3)$, depending on the Au coverage in accordance with previous studies. The highest coverage phase is observed to be mixed with a $(4,0)\times(\bar{3},3)$ phase. ARP spectra show no clear surface-state bands on the 1×2 surface within the bulk band gap. The 2×5 surface composed of one-dimensional (1D) atomic chain exhibits two dispersive metallic bands with exact quarter and half fillings. Their Fermi surfaces are straight lines within the experimental accuracy indicating strong 1D characters. This phase is thus one of the most ideal 1D metallic systems ever fabricated on solid surfaces. The $(4,0)\times(\bar{1},3)$ surface has only one strongly dispersing but semiconducting band following the $\times2$ periodicity apparently.

DOI: 10.1103/PhysRevB.78.075315 PACS number(s): 73.20.At, 79.60.Dp, 68.43.Hn

I. INTRODUCTION

One-dimensional (1D) physics in solids is more intriguing than in higher dimension due to enhanced many-body interactions. The density wave formation and the breakdown of the Fermi-liquid behavior are among well-known consequences of such interactions.[1–3] In recent years, it was reported that the self-assembled atomic wire arrays on silicon surfaces exhibit well-ordered atomic structures and quasi-1D metallic band structures. The examples are Si(111)4×1-In, Si(553)$4\frac{1}{3}\times2$-Au, Si(557)$5\frac{2}{3}\times2$-Au, and Si(5512)$8\frac{2}{3}\times2$-Au surfaces,[4–9] where the interwire spacings are 1.33, 1.48, 1.92, and 3.14 nm, respectively.[10] Peierls-type metal-insulator transitions were observed on these surfaces due probably to the 1D metallic bands satisfying proper Fermi-surface (FS) nesting conditions for the strong electron-phonon coupling.

More recently, another Au-induced atomic wire array with an interwire spacing of 2.72 nm was found on Si(110) with a unit cell of 2×5.[11] The similarity of the overall atomic structure with double atomic rows to Si(557)$5\frac{2}{3}\times2$-Au was suggested in the scanning tunneling microscopy (STM) observation.[11] Since we follow the conventional notation of the unit cells on the Si(110) surface, the $\times2$ directions—which are commonly along the atomic wires—are literally opposite. While the atomic structure of these wires are unclear, two parabolic bands approaching the Fermi energy (E_F) with band fillings of a half and roughly a third were reported by angle-resolved photoemission (ARP) along the wire direction.[11] However, the detailed density of states (DOS) at E_F and the FS were not presented, leaving the metallic nature and the dimensionality of these bands unclear. If these two bands are 1D metallic bands, then one may expect to observe interesting phenomena such as the coexistence of $\times2$ and $\times3$ Peierls distortions in Si(553)$4\frac{1}{3}\times2$-Au. On the other hand, the earlier reflection high-energy electron diffraction (RHEED) study found three Au-induced phases on the Si(110) surface depending on the Au coverage; the 1×2 phase at ~0.2 monolayer (ML), 2×5 at around 0.4 ML, and $(4,0)\times(\bar{1},3)$ at higher coverages up to 1 ML.[12] However, atomic and electronic structures of the 1×2 and the $(4,0)\times(\bar{1},3)$ phases are veiled.

In the present work, we systematically investigate the evolution of the phases on the Au/Si(110) surface and characterize their electronic band structures using low-energy electron diffraction (LEED) and ARP. This system shows three well-ordered phases as a function of the Au coverage in overall agreement with the previous work.[12] The 1×2 surface does not exhibit any dispersive surface-state band. The highest coverage phase is shown to be a mixed phase of $(4,0)\times(\bar{1},3)$ and $(4,0)\times(\bar{3},3)$, for which only a single strongly dispersing but semiconducting band is observed. The 2×5 surface shows two metallic surface-state bands, which disperse one-dimensionally along the wire direction with electron fillings of a quarter and a half. This result partly disagrees with the previous ARP work.[11] The ideal 1D metallic property of the partially filled bands are confirmed from the FS mapping. The 2×5 surface is promising for further studies on the low-temperature physics of 1D metals.

II. EXPERIMENT

The ARP measurements were performed using a high-resolution electron analyzer (SES-100, Gamma Data, Sweden) with a high-flux discharge lamp and a toroidal grating monochromator. The He I radiation ($h\nu$=21.2 eV) was used to excite photoelectrons at a base pressure better than 1×10^{-10} torr. The nominal energy and angular resolutions were 20 meV and 0.15°, respectively. The mapping of FSs and band dispersions was performed by rotating the sample along two orthogonal polar axes. The sample was cryogenically cooled down to 90 K as the temperature was monitored by a calibrated resistance sensor. Well-ordered Si(110) clean surfaces were prepared by repeated cycles of flashing at 1500 K and subsequent annealing at 870 K for 10 min followed by slowly cooling down to room temperature (RT). This procedure produced a well defined 16×2 double-domain LEED pattern, as shown in Fig. 1(a). The 16×2 reconstruction

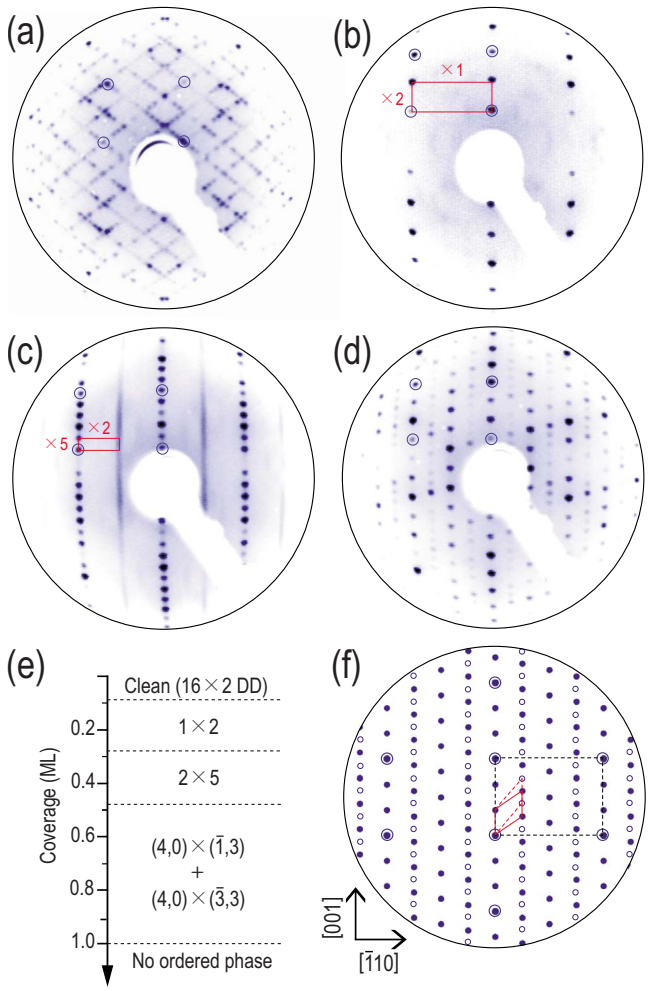

FIG. 1. (Color online) LEED patterns of the Au/Si(110) surface as a function of Au coverage (Θ) taken with a beam energy of 90 eV and at RT. (a) The clean Si(110)16×2 surface, (b) the 1×2 phase at $\Theta \sim 0.2$ ML, (c) 2×5 at $\Theta \sim 0.4$ ML, (d) $(4,0)\times(\bar{1},3)$ mixed with $(4,0)\times(\bar{3},3)$ at $\Theta \sim 1$ ML, and (f) its schematic representation. The 1×1 spots are depicted by open circles. The phase diagram is summarized in (e).

typically exhibits a structure with atomic rows running along two directions, $[\bar{1}12]$ and $[1\bar{1}2]$, containing up and down terraces separated by monatomic height steps.[13–15] This phase exhibits two insulating bands at around 0.4 and 0.9 eV below E_F.[16] An Au-coated W filament was used as the evaporating source. The temperature of the sample during the deposition of Au was held at 870 K followed by annealing at the same temperature.[12] The phase formation was investigated using a LEED optics with a charge coupled device camera. The deposition rate of the evaporator was calibrated by a well established phase diagram of Au/Si(111). The coverage dependent phase changes were consistent with the earlier study, which measured the Au coverage quantitatively by the x-ray total reflection excited by a high-energy electron beam.[12]

III. RESULTS AND DISCUSSION

A. LEED observation

According to the phase diagram derived by the previous RHEED study,[12] there are three ordered phases: 1×2, 2×5, and $(4,0)\times(\bar{1},3)$. In this phase diagram, as Au of 0.18 ML is deposited on the clean Si(110) surface, the 1×2 phase is optimized at the annealing temperature between 810 and 1240 K. When 0.37 ML is deposited, the 2×5 phase is optimized at 810~1020 K. Between 0.5 and 1 ML the $(4,0)\times(\bar{1},3)$ phase is well developed at 710~1120 K. At above 1240 K, all phases were reported to transform into a 1×1 phase.

Figures 1(b)–1(d) show the LEED patterns of the Au-induced superstructures. The corresponding unit cells are depicted by solid lines. The fundamental (1×1) LEED spots of the bare Si(110) surface are marked by large open circles. The evaporation of 0.2 ML of Au followed by annealing at 870~950 K resulted in a sharp *single domain* 1×2 LEED pattern (×2 spots along the [001] direction) as shown in Fig. 1(b). This indicates that the small amount of Au adsorbates changes the step morphology of the surface drastically.

By increasing the Au coverage to 0.4 ML, the 1×2 phase evolves into a well defined single domain 2×5 phase at the same temperature range as the 1×2 phase. The LEED pattern in Fig. 1(c) shows the strong ×2 streaks, which indicate anisotropic 2×5 domains along the $[\bar{1}10]$ direction with a weak lateral coherence along the [001] direction. The ×2 order was also noticed in STM, which shows a rather well-ordered atomic wire array with an intrawire ×2 structure.[11] Similar ×2 modulations were also observed in LEED and STM studies of the Au/Si(553) and the Au/Si(557) surface.[17,18] The Au/Si(111) system also reveals a very similar 5×2 LEED pattern but with a smaller unit-cell size.[19]

Finally, at a higher Au coverage than 0.5 ML up to 1 ML a new phase is observed, as shown in Fig. 1(d). Unlike the earlier study,[12] this phase consists of two different phases: One is the $(4,0)\times(\bar{1},3)$ phase [dashed lines and open circles in Figs. 1(d) and 1(f)] as reported in the previous study;[12] and the other, although its LEED spots are weaker, is the $(4,0)\times(\bar{3},3)$ phase as marked by solid lines and symbols. The isolated $(4,0)\times(\bar{1},3)$ phase could not be prepared throughout various different coverages and annealing temperatures. The $(4,0)\times(\bar{3},3)$ phase may not be resolved in the previous RHEED study due to its weak diffraction intensity. This mixed phase is called "4×3" hereafter for simplicity. Above the Au coverage of 1 ML, no ordered phase is found. The phase diagram deduced from the LEED observation is summarized in Fig. 1(e).

B. ARP study: An overview

We measured the electronic band dispersions of all well-ordered surface phases confirmed by the LEED observation. Qualitatively speaking, the electronic structure of this system evolves from a semiconducting phase into a metallic one and finally develops into another semiconducting one as the Au coverage increases. The measured band dispersions are

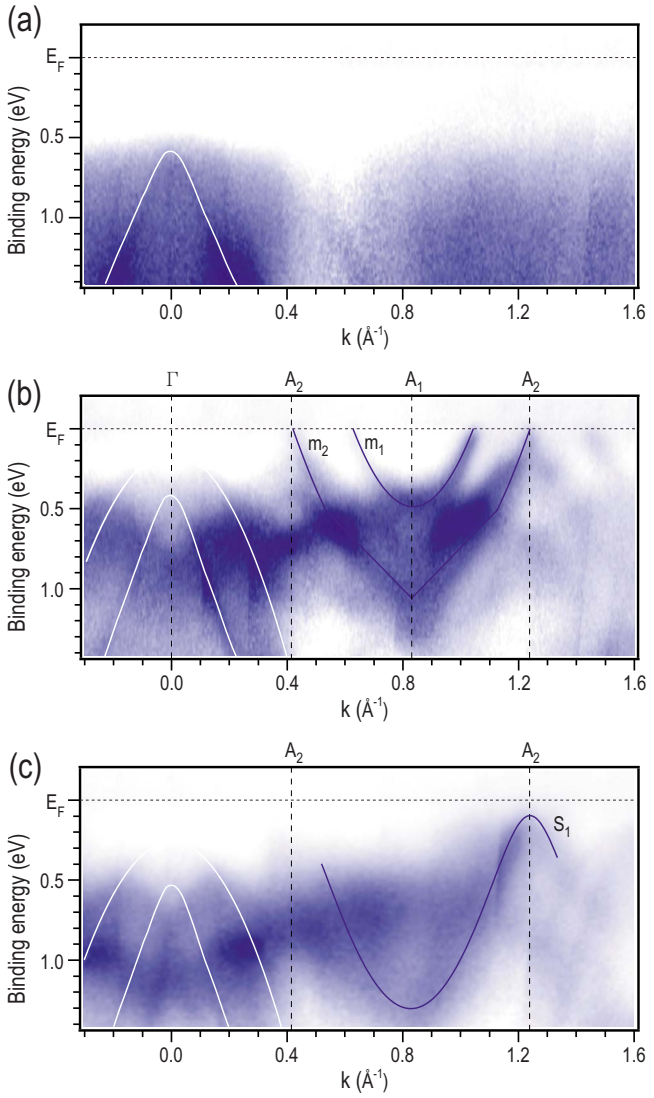

FIG. 2. (Color online) ARP intensity maps taken along the $[\bar{1}10]$ direction for (a) the 1×2, (b) the 2×5, and (c) the 4×3 phases. The prominent surface-state and bulk bands are guided roughly by dark and white solid lines, respectively. The zone boundary of the $n\times2$ ($n\times1$) unit cell at 0.41 and 1.23 Å^{-1} (0.82 Å^{-1}) is labeled as A_2 (A_1).

shown in Figs. 2(a)–2(c). All dispersions are measured along the $[\bar{1}10]$ direction. The ARP intensity is plotted in a blue (gray) scale with a higher intensity in the darker contrast. The dispersions of prominent features are roughly guided by solid lines in Figs. 2(b) and 2(c). The bulk bands are marked by white lines. The energy shifts of the bulk bands noticed in Figs. 2(a)–2(c), especially for the 2×5 phase, came from the band bending caused by the Fermi-level pinning due to metallic surface states.

Figure 2(a) shows the band dispersion of the 1×2 phase formed at the lowest Au coverage taken at RT. There is no dispersive feature except for weak bulk band emissions around the normal emission ($k=0$). No DOS is detected around E_F indicating clearly the semiconducting or insulating nature. Instead, diffuse photoelectron intensities are observed throughout the bulk band-gap region away from E_F.

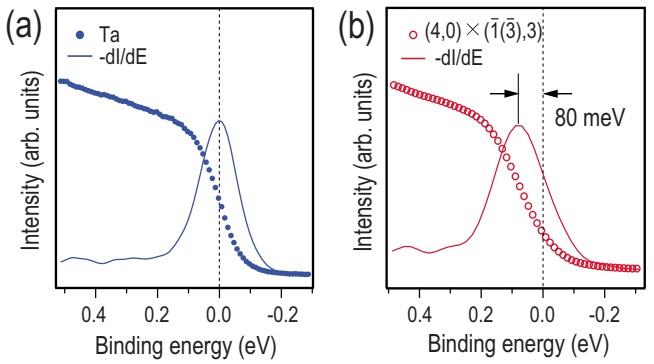

FIG. 3. (Color online) ARP EDCs around the Fermi energy of (a) polycrystalline Ta (closed circle) and (b) the 4×3 phase (open circle) at the A_2 point (the $\times2$ SBZ boundary). The derivatives of the EDCs (solid lines) are given together to quantify the leading edges.

This suggests that the surface may be disordered in contrast to its sharp 1×2 LEED pattern. The possible local surface disorder cannot be confirmed without a proper STM study, which is not available now.

In sharp contrast to the 1×2 phase, the 2×5 phase exhibits very well resolved surface-state bands. The band map in Fig. 2(b) was taken at 90 K for better resolution, but it is basically identical to that taken at RT except for the reduced thermal broadening. As roughly guided by solid lines, there exist at least two metallic bands, m_1 and m_2, centered at the $\times1$ surface Brillouin-zone (SBZ) boundary (A_1). The detailed and extensive discussion of this band structure will be given in the next section.

The surface phase formed at the highest coverage of Au is the 4×3 mixed phase. The band dispersion of this phase optimized at ~1 ML is shown in Fig. 2(c). There is no metallic band but a semiconducting band S_1 with a strong dispersion. The bandwidth is 1.22 eV. Since its band top is quite close to E_F, the band gap, if any, needs to be checked more carefully. The gap size for the S_1 band is derived from the ARP energy distribution curve (EDC) at the $\times2$ SBZ boundary A_2, as shown in Fig. 3. Since there is no well defined quasiparticle peak, we estimate the gap size below E_F using the leading edge method.[20] The leading edge centers of EDCs are determined by the derivatives of the spectra (solid lines). This leading edge center position agrees well with E_F for the normal-metal Ta sample but deviates by 80 meV for the S_1 band. From this and the band dispersion given in Fig. 2(c), one can confirm that the band gap of S_1 below E_F is 80 meV. In spite of the sharp $\times4$ periodicity along the $[\bar{1}10]$ direction in the LEED pattern, the band dispersion does not reflect this periodicity but follows only the $\times2$ periodicity. It is not clear at present whether the lack of the $\times4$ periodicity is due to the mixed surface domains of $(4,0)\times(\bar{1},3)$ and $(4,0)\times(\bar{3},3)$ or due to the weak $\times4$ potential compared to that of a $\times2$. According to a recent study,[21] for a quasi-1D electronic system under two competing periodic potentials, the ARP spectral weight concentrates mainly on the bands following the dominant potential. A similar effect has also been observed in a 2D electronic system of Pb/Si(111).[22]

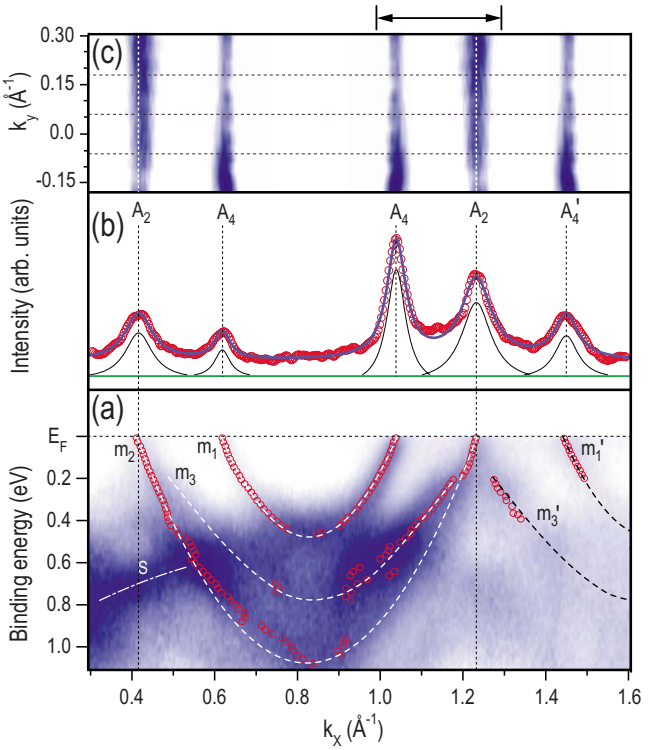

FIG. 4. (Color online) (a) Enlarged ARP intensity map from Fig. 2(b) for the metallic surface states of the 2×5 phase. The spectral peak positions given in circles are quantitatively determined from Lorentzian fits of the MDCs of the spectral intensity. These peak positions are then fitted with simple parabolic functions as shown by dashed lines. (b) The MDC at the Fermi energy (E_F) fitted with five Lorentzian curves after removing a linear background (the straight line at the bottom), which show the E_F crossings of m_1 and m_2 bands. The result of the fit is given as the solid curve overlaid on the raw data (circles). The crossings of m_2 are located exactly at the $\times2$ SBZ boundaries (A_2). (c) The ARP intensity map at E_F as functions of k_x and k_y, where k_x runs along $[\bar{1}10]$ (the atomic wires), which shows the 1D Fermi contours of m_1 and m_2. The experimental data are taken for the arrowed range only and expanded according to the translational symmetry of the surface.

One more thing to be mentioned on this phase is that its overall ARP intensity distribution is similar to that of the 2×5 phase. One may also find some similarity between the m_2 and the S_1 bands. This may indicate the similarity in the local building block structures of these two phases, while an STM study is requested.

C. ARP study: The 1D metallic phase of 2×5

As overviewed above, although LEED indicates three well-ordered surface phases on the Au/Si(110) system, only the 2×5 phase exhibits a rich band structure with dispersing and metallic bands. In order to inspect closely the detailed band dispersions of this phase, the enlarged ARP intensity map for the bulk band-gap region is shown in Fig. 4(a). The photoemission intensities as a function of momentum or momentum distribution curves (MDCs) exhibit very sharp well defined peaks shown partly in Fig. 4(b). Since the MDC is not affected by the Fermi-Dirac function, one can, in principle, track a spectral feature all the way up to E_F.[23] In Fig. 4(b), the MDC at E_F (open circles) is fitted by five Lorentzian functions with full width at half maxima of 0.09, 0.05, 0.05, 0.08, and 0.06 Å^{-1}, from left to right peaks. These peaks correspond to the E_F crossings of m_1 and m_2 bands. The peak positions derived from many such MDC fits are shown as open circles in Fig. 4(a). A few other spectral features are noticed in this way. Basically, there are four dominating features; two metallic bands (m_1 and m_2) crossing E_F and two insulating bands (m_3 and S). The intensity of m_2 is dominating around $k_x=0.5-0.6$ Å^{-1} and that of m_3 dominating around $k_x=0.9-1.0$ Å^{-1} to yield a large asymmetry around the center of the $\times1$ SBZ (A_1). Two rather weak features m_1' and m_3' are also noticed near E_F at the second SBZ. The dispersions of the spectral features dispersing toward E_F are then fitted by simple parabolas as indicated by dashed lines. The m_3 band does not cross E_F but is folded at the $\times2$ SBZ boundary (A_2) to become m_3'. This semiconducting nature and the band gap at A_2 for m_3 will be made clearer below (from the EDC analysis). The parabolic bands m_1 and m_2 reach E_F at $k_x=0.41(1.23)$ and $0.62(1.03)$ Å^{-1}, respectively. Thus, the electron fillings of m_1 and m_2 bands are measured to be 0.25 and 0.50, respectively, where one represents a fully filled band. These band fillings (quarter and half) are reliable within the accuracy of our measurement (±0.02 Å^{-1} or 1/50 in the band filling). The parabolic fits of the dispersions [dashed lines in Fig. 4(a)] yield the effective mass (m^*) values of $0.35m_e$ and $0.59m_e$ (m_e the free-electron mass) for m_1 and m_2, respectively. The dispersion of m_1' (m_3') is identical to m_1 (m_3) with the same effective mass indicating that it is the folded (or umklapp) branch of m_1 (m_3) following the $\times2$ periodicity. The significantly weaker intensities of m_1' and m_3' further support the assignment as folded (or umklapp) bands. Since all these bands are located well within the bulk band gap, they are unambiguously assigned as surface-state bands.

The momentum distribution map of the ARP intensity at E_F is shown in Fig. 4(c), which reveals the Fermi contours of m_1 and m_2 bands. The raw data, taken only in a part of SBZ as marked by the arrows, are mirror symmetrized across the $[\bar{1}10]$ direction reflecting the symmetry confirmed by LEED. They show very straight lines without any noticeable wiggling within the experimental accuracy. This indicates that the metallic surface states, m_1 and m_2, are ideally 1D with only a negligible interwire or two-dimensional (2D) coupling. The ratio of intrawire and interwire coupling strengths can be quantified by a tight-binding fit of Fermi contours, which is larger than 100.[9]

Figure 5 shows the EDCs of m_1 and m_2 bands at their E_F crossings on A_4 and A_2 indicated in Fig. 4, respectively. The spectrum of a polycrystalline Ta sheet is included to confirm the metallicity. In Fig. 5(a), the EDC of the m_1 band (open circles) obviously exhibits a huge quasiparticle peak with a clear metallic edge. The EDC at A_2 shows two small but distinctive peaks corresponding to m_2 and m_3 bands in Fig. 5(b). The m_3 band splits from m_2 by about 160 meV indicating its apparent semiconducting property in contrast to m_2. The band gap of m_3 is larger than 240 meV, while we do not

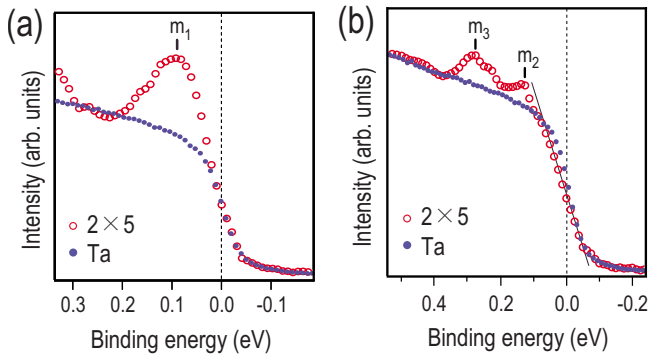

FIG. 5. (Color online) EDCs near the Fermi energy of (a) m_1 and (b) m_2 (m_3) (open circle) bands of the 2×5 surface at the corresponding Fermi wave vectors. The EDC of a polycrystalline Ta sheet (solid circles) is given together for comparison. The solid line in (b) guides the leading edge of the m_2 band showing a subtle deviation from the normal metallic edge.

know its gap size above E_F. A very subtle deviation from the normal metallic behavior is noticed for the m_2 band; the slight deviation of its Fermi edge (guided by a straight line) from that of Ta. It is not clear whether this is due to an unquantified small band gap or other effects such as disorder or non-Fermi-liquid behavior. Note also that the m_2 band has no folded or umklapp band feature following the $\times2$ periodicity in contrast to m_1 and m_3. That is, the m_2 band seems to follow only the $\times1$ periodicity. These rather mysterious spectral behaviors of m_2 are reproduced for a few different samples measured in the present work. A higher-resolution ARP measurement at a lower temperature and a high-resolution STM study may be helpful to understand these issues.

The band dispersions of the 2×5 phase measured here are partly different from the previous ARP study.[11] First, the previous study did not see the m_3 band. Second, the band filling of m_1 was estimated about one-third instead of a quarter, while the existence of a half-filled band (m_2) is consistent. We note that the previous MDC at E_F is very broad, not providing clearly resolved peaks for m_1 and m_2. This broadening may have made the quantification of the exact band filling and the identification of m_3 resolved from m_2 difficult. This broad MDC is thought to be possibly due to an ill-optimized surface phase based on our own practice. Indeed, we could reproduce very similar band dispersions to those reported at a slightly higher coverage than the present 2×5 phase, where the LEED pattern shows broad $\times4$ features. The previous RHEED study also indicated that the phase formation is sensitive to the annealing temperature and the Au coverage.[12]

It is worthwhile to compare the metallic band structure of Au/Si(110) with those of the other Au-induced 1D phases on flat or vicinal Si(111) surfaces such as Si(111), Si(553), Si(557), and Si(5 5 12). The band structures of Si(557) and Si(5 5 12) are almost identical with two nearly half-filled bands.[6,7,9] That of Si(553) also shares these two nearly half-filled bands but there exists an extra band with a band filling between one-third and a quarter.[5,8] The Si(111)5×2-Au surface also has a similar partially filled band.[24] However, the filling of this band depends on the density of Si adatoms intrinsic to this surface; the band filling can increase from 0.3 but a band gap forms before it reaches the one-third filling.[24] This surface also has a counterpart of the half-filled band but it has a rather large band gap without the splitting in contrast to the half-filled bands on the vicinal surfaces.[24] The band structure of Si(110)2×5-Au looks similar to that of Si(553)-Au with multiple partially filled bands. Furthermore, the effective masses of the metallic bands are also very close; $0.3m_e$ and $0.65m_e$ for nearly one-third and nearly half-filled bands on Si(553)-Au, respectively,[9] and $0.35m_e$ and $0.59m_e$ for m_1 and m_2, respectively, on Au/Si(110). However, the exact quarter filling (m_1) and the lack of the splitting in the half-filled band (m_2) are unique for the present system.

As for the splitting of the half-filled bands of Au/Si(553) and Au/Si(557), recent theoretical and experimental studies suggested the spin-orbit interaction origin, the Rashba effect due to the strong contribution of Au p electrons.[25,26] It is thus notable that the present system does not exhibit such a splitting. The two bands, m_2 and m_3, with similar dispersions observed here bear little resemblance with the spin-orbit split bands. However, for a further discussion of this interesting difference, the detailed structural information on the present system is highly requested.

There exist further differences between these surfaces. For the cases of Au/Si(553), Au/Si(557), and Au/Si(5 5 12), the nearly half-filled bands and the nearly one-third filled band result in the Peierls-type distortions of $\times2$ and $\times3$ periodicities, respectively, with band-gap openings.[5–7] The corresponding transition temperatures are as high as 200–300 K. However, on the Si(110)2×5-Au surface, we could not observe any sign of phase transitions down to the temperature of 90 K. This contrasting behavior is unexpected considering the more exact band fillings compatible with a commensurate lattice distortions and the more ideal 1D dispersions of Si(110)2×5-Au. The ratio of intrawire and interwire couplings in the present system is larger than 100 as mentioned above, which can be compared to those of Au/Si(553), 12 (nearly third-filled band) or ~40 (half-filled splitting bands), and of Au/Si(557) larger than 60 (half-filled bands).[9] Although the corresponding values for Au/Si(5 5 12) and Au/Si(111) were not reported yet, these values seem to scale with the interwire distance of 1.5, 1.9, and 2.7 nm for Au/Si(553), Au/Si(557), and Au/Si(110), respectively. That is, the Si(110)2×5-Au surface has one of the largest unit-cell size perpendicular to the metallic atomic wires to yield one of the most ideal 1D metallic band structures. It is thus a very interesting question that what kind of ground states the present system would have. The quarter-filled bands were reported in 1D organic compounds such as Bechgaard salts and TTF-TCNQ and also in inorganic 1D systems such as $NbSe_3$.[27–29] These systems exhibit various density wave ground states and non-Fermi-liquid behaviors such as the spin charge separation.[28,30] The search for an exotic ground state for the present system at a low temperature is promising but is left as a forthcoming project.

IV. CONCLUSIONS

The phase formation and the electronic band structures of Au-induced superstructures on the Si(110) surface are sys-

tematically studied as a function of the Au coverage using LEED and ARP. At a low coverage of ~0.2 ML, the LEED pattern shows a well-ordered 1×2 phase. However, this phase exhibits only diffuse ARP intensities without any well defined surface state. The possibility of a locally disordered surface structure is, thus, raised. No ARP intensity is detected near E_F indicating a semiconducting or an insulating nature of this phase. At the coverage of ~0.4 ML, a well defined 2×5 phase appears, which exhibits highly dispersive and well resolved surface-state bands. This surface phase was shown to feature a 1D atomic wire structure in the previous STM study. The 2×5 phase has two metallic bands (m_1 and m_2) with exact quarter-electron and half-electron fillings and one insulating band (m_3) with a band gap of 240 meV below E_F. While the m_1 and m_3 bands follow the $\times2$ surface periodicity, as indicated by the band back foldings or the umklapp bands, the m_2 band follows only the apparent $\times1$ periodicity. The exact quarter filling and the lack of the splitting of the half-filled band are contrasted with the similar 1D metallic bands of other Au-induced 1D structures on Si(557), Si(553), and Si(5 5 12). The Fermi contours of m_1 and m_2 bands show a highly 1D topology with stronger anisotropy than the similar systems on Si(557) and Si(553) surfaces. This can be understood from the larger interwire distance in the present system. At up to 1 ML a $(4,0)\times(\bar{1},3)$ phase mixed with minor $(4,0)\times(\bar{3},3)$ domains (called 4×3) is observed with a clear LEED pattern, which exhibits a highly dispersive but semiconducting surface-state band with a small band gap of 80 meV below E_F. The unique quarter-filled band and the ideal 1D Fermi contours of the Si(110)2×5-Au surface makes this system promising for the search of an exotic ground-state properties of a 1D electronic system[31] at a sufficiently low temperature.

ACKNOWLEDGMENTS

This work was supported by KOSEF through the Center for Atomic Wires and Layers of the CRi program.

*yeom@yonsei.ac.kr

[1] R. F. Peierls, *Quantum Theory of Solids* (Clarendon, Oxford, 1955).
[2] G. Grüner, *Density Waves in Solids* (Addison-Wesley, Massachusetts, 1994).
[3] T. Giamarchi, *Quantum Physics in One Dimension* (Clarendon, Oxford, 2004).
[4] H. W. Yeom, S. Takeda, E. Rotenberg, I. Matsuda, K. Horikoshi, J. Schaefer, C. M. Lee, S. D. Kevan, T. Ohta, T. Nagao, and S. Hasegawa, Phys. Rev. Lett. **82**, 4898 (1999).
[5] J. R. Ahn, P. G. Kang, K. D. Ryang, and H. W. Yeom, Phys. Rev. Lett. **95**, 196402 (2005).
[6] J. R. Ahn, H. W. Yeom, H. S. Yoon, and I.-W. Lyo, Phys. Rev. Lett. **91**, 196403 (2003).
[7] J. R. Ahn, H. W. Yeom, E. S. Cho, and C. Y. Park, Phys. Rev. B **69**, 233311 (2004).
[8] J. N. Crain, A. Kirakosian, K. N. Altmann, C. Bromberger, S. C. Erwin, J. L. McChesney, J.-L. Lin, and F. J. Himpsel, Phys. Rev. Lett. **90**, 176805 (2003).
[9] J. N. Crain, J. L. McChesney, F. Zheng, M. C. Gallagher, P. C. Snijders, M. Bissen, C. Gundelach, S. C. Erwin, and F. J. Himpsel, Phys. Rev. B **69**, 125401 (2004).
[10] The vicinal surfaces are all based on Si(111) and thus the unit-cell sizes are referred to that of the bulk terminated Si(111)1×1 surface.
[11] J. L. McChesney, J. N. Crain, F. J. Himpsel, and R. Bennewitz, Phys. Rev. B **72**, 035446 (2005).
[12] Y. Yamamoto, Surf. Sci. **271**, 407 (1992).
[13] A. A. Stekolnikov, J. Furthmüller, and F. Bechstedt, Phys. Rev. Lett. **93**, 136104 (2004).
[14] A. Cricenti, B. Nesterenko, P. Perfetti, G. LeLay, and C. Sebenne, J. Vac. Sci. Technol. A **14**, 2448 (1996).
[15] T. An, M. Yoshimura, I. Ono, and K. Ueda, Phys. Rev. B **61**, 3006 (2000).
[16] N. D. Kim, Y. K. Kim, C.-Y. Park, H. W. Yeom, H. Koh, E. Rotenberg, and J. R. Ahn, Phys. Rev. B **75**, 125309 (2007).
[17] K.-D. Ryang, P. G. Kang, H. W. Yeom, and S. Jeong, Phys. Rev. B **76**, 205325 (2007).
[18] H. W. Yeom, J. R. Ahn, H. S. Yoon, I.-W. Lyo, H. Jeong, and S. Jeong, Phys. Rev. B **72**, 035323 (2005).
[19] J. L. McChesney, J. N. Crain, V. Pérez-Dieste, F. Zheng, M. C. Gallagher, M. Bissen, C. Gundelach, and F. J. Himpsel, Phys. Rev. B **70**, 195430 (2004).
[20] T. Yokoya, T. Kiss, A. Chainani, S. Shin, M. Nohara, and H. Takagi, Science **294**, 2518 (2001).
[21] J. Voit, L. Perfetti, F. Zwick, H. Berger, G. Magaritondo, G. Grüner, H. Höchst, and M. Grioni, Science **290**, 501 (2000).
[22] W. H. Choi, H. Koh, E. Rotenberg, and H. W. Yeom, Phys. Rev. B **75**, 075329 (2007).
[23] T. Hirahara, I. Matsuda, M. Ueno, and S. Hasegawa, Surf. Sci. **563**, 191 (2004).
[24] W. H. Choi, P. G. Kang, K. D. Ryang, and H. W. Yeom, Phys. Rev. Lett. **100**, 126801 (2008).
[25] D. Sánchez-Portal, S. Riikonen, and R. M. Martin, Phys. Rev. Lett. **93**, 146803 (2004).
[26] I. Barke, Fan Zheng, T. K. Rügheimer, and F. J. Himpsel, Phys. Rev. Lett. **97**, 226405 (2006).
[27] F. Zwick, S. Brown, G. Margaritondo, C. Merlic, M. Onellion, J. Voit, and M. Grioni, Phys. Rev. Lett. **79**, 3982 (1997).
[28] R. Claessen, M. Sing, U. Schwingenschlögl, P. Blaha, M. Dressel, and C. S. Jacobsen, Phys. Rev. Lett. **88**, 096402 (2002).
[29] J. Schäfer, Eli Rotenberg, S. D. Kevan, P. Blaha, R. Claessen, and R. E. Thorne, Phys. Rev. Lett. **87**, 196403 (2001).
[30] T. Lorenz, M. Hofmann, M. Grüninger, A. Freimuth, G. S. Uhrig, M. Dumm, and M. Dressel, Nature (London) **418**, 614 (2002).
[31] H. Steinberg, G. Barak, A. Yacoby, L. N. Pfeiffer, K. W. West, B. I. Halperin, and K. L. Hur, Nat. Phys. **4**, 116 (2008).